materials

MDPI

Article

Human Bone-Marrow-Derived Stem-Cell-Seeded 3D Chitosan–Gelatin–Genipin Scaffolds Show Enhanced Extracellular Matrix Mineralization When Cultured under a Perfusion Flow in Osteogenic Medium

Gabriele Boretti [1], Emanuele Giordano [2,3,*], Mariana Ionita [4,5,6], George Mihail Vlasceanu [4,5], Ólafur Eysteinn Sigurjónsson [1,7], Paolo Gargiulo [1,8] and Joseph Lovecchio [1,8]

1 School of Science and Engineering, Reykjavík University, 102 Reykjavík, Iceland; gabriele23@ru.is (G.B.); oes@ru.is (Ó.E.S.); paolo@ru.is (P.G.); josephl@ru.is (J.L.)
2 Laboratory of Cellular and Molecular Engineering "Silvio Cavalcanti", Department of Electrical, Electronic and Information Engineering "Guglielmo Marconi" (DEI), University of Bologna, 47522 Cesena, FC, Italy
3 Advanced Research Center on Electronic Systems (ARCES), University of Bologna, 40126 Bologna, BO, Italy
4 Faculty of Medical Engineering, University Politehnica of Bucharest, 060042 Bucharest, Romania; mariana.ionita@polimi.it (M.I.); vlasceanu.georgemihail@yahoo.ro (G.M.V.)
5 Advanced Polymer Materials Group, University Politehnica of Bucharest, 060042 Bucharest, Romania
6 eBio-Hub Research Centre, University Politehnica of Bucharest-Campus, 060042 Bucharest, Romania
7 The Blood Bank, Landspitali, The National University Hospital of Iceland, 105 Reykjavík, Iceland
8 Institute of Biomedical and Neural Engineering, Reykjavik University, 102 Reykjavík, Iceland
* Correspondence: emanuele.giordano@unibo.it

Citation: Boretti, G.; Giordano, E.; Ionita, M.; Vlasceanu, G.M.; Sigurjónsson, Ó.E.; Gargiulo, P.; Lovecchio, J. Human Bone-Marrow-Derived Stem-Cell-Seeded 3D Chitosan–Gelatin–Genipin Scaffolds Show Enhanced Extracellular Matrix Mineralization When Cultured under a Perfusion Flow in Osteogenic Medium. *Materials* **2023**, *16*, 5898. https://doi.org/10.3390/ma16175898

Academic Editor: Franz E. Weber

Received: 7 July 2023
Revised: 2 August 2023
Accepted: 7 August 2023
Published: 29 August 2023

Abstract: Tissue-engineered bone tissue grafts are a promising alternative to the more conventional use of natural donor bone grafts. However, choosing an appropriate biomaterial/scaffold to sustain cell survival, proliferation, and differentiation in a 3D environment remains one of the most critical issues in this domain. Recently, chitosan/gelatin/genipin (CGG) hybrid scaffolds have been proven as a more suitable environment to induce osteogenic commitment in undifferentiated cells when doped with graphene oxide (GO). Some concern is, however, raised towards the use of graphene and graphene-related material in medical applications. The purpose of this work was thus to check if the osteogenic potential of CGG scaffolds without added GO could be increased by improving the medium diffusion in a 3D culture of differentiating cells. To this aim, the level of extracellular matrix (ECM) mineralization was evaluated in human bone-marrow-derived stem cell (hBMSC)-seeded 3D CGG scaffolds upon culture under a perfusion flow in a dedicated custom-made bioreactor system. One week after initiating dynamic culture, histological/histochemical evaluations of CGG scaffolds were carried out to analyze the early osteogenic commitment of the culture. The analyses show the enhanced ECM mineralization of the 3D perfused culture compared to the static counterpart. The results of this investigation reveal a new perspective on more efficient clinical applications of CGG scaffolds without added GO.

Keywords: biomaterials; bioreactors; chitosan; gelatin; graphene oxide; human bone-marrow-derived mesenchymal stem cells; regenerative medicine; scaffolds; tissue engineering

1. Introduction

Tissue-engineered bone tissue grafts are viewed as a promising alternative to the conventional use of natural donor bone grafts in terms of protocol standardization, but their effective translation into clinical practice is still a challenge [1–4]. In particular, choosing an appropriate biomaterial/scaffold to sustain cell survival, proliferation and differentiation in a 3D environment remains one of the most critical aspects to approach [5,6]. Several natural or synthetic biomaterials have been used to this aim [7–14]. In this respect, we

recently proposed chitosan/gelatin/genipin (CGG) hybrid scaffolds doped/reinforced with graphene oxide (GO) as a promising biomaterial/scaffold with osteogenic potential [15]. Some concern was however raised towards the use of graphene and graphene-related material in medical applications, requiring further testing and full understanding of their behavior in biological systems [16,17]. While the results of such studies are ongoing, we here thus propose to evaluate the osteogenic potential of CGG scaffolds [18,19] without added GO, by including a perfusion flow into the differentiation-inducing protocol. In fact, it is well established that a dynamic environment can improve diffusion gradients, especially within tridimensional tissue constructs, and thus enhance their functional behavior. Indeed, several studies [20–26] demonstrated that the use of bioreactor systems to this aim can improve cell phenotype commitment. Thus, here, human bone-marrow-derived stem cell (hBMSC)-seeded 3D CGG scaffolds have been cultured under a perfusion flow and the extent of the early osteogenic process [27–32] has been evaluated as the level of extracellular matrix (ECM) mineralization was measured. An increased ECM mineralization was found in 3D CGG scaffolds cultured in dynamic conditions compared to static conditions. The results of this investigation reveal a new perspective on potential clinical applications of CGG scaffolds without added GO.

2. Materials and Methods

2.1. Three-Dimensional Chitosan–Gelatin–Genipin Scaffolds

Crab-shell-derived medium-molecular-weight chitosan with a 75–85% deacetylation degree, cold water fish gelatin, genipin (purity > 98%—HPLC grade), and acetic acid (>99.7%) were purchased from Sigma Aldrich (St. Louis, MO, USA) and used without prior purification. The composites' synthesis was carried out in double distilled water. Genipin crosslinked gelatin/chitosan blend scaffolds were prepared under identical conditions as previously reported [33]. Briefly, gelatin was dissolved in water (5% *w/v*) by thoroughly stirring at 50 °C for 1 h and mixed with a 1% wt. chitosan solution prepared in a mild acidic solution (1% *v/v*) by stirring overnight at 40 °C. For a total of 50 mL of solution, 8.33 mL of gelatin solution was homogenized with 41.67 mL chitosan solution. The crosslinking was carried out with genipin (1% *w/w* in water). Next, materials were frozen at −80 °C and freeze-dried (−55 °C).

2.2. Perfusion Bioreactor

A perfusion bioreactor system was used to generate a continuous perfusion flow in a range of 0.25 to 1 mL/min, aiming at obtaining a constant supply of nutrients and the removal of waste products to sustain the 3D cell culture [34–36]. The device consists of (i) a unibody plastic case (190 L, 240 W, and 90 H mm in dimension); (ii) two autoclavable WPM2-S1EACP peristaltic pumps (WELCO, Tokyo, Japan); (iii) an appropriate set of 3D printed culture plates. A control unit hosting an Arduino UNO, two EasyDriver stepper motor drivers (SparkFun Electronics, Boulder, CO, USA), and a PMB-12V35W1AA power supply (Delta Electronics, Taipei, Taiwan) was designed to guide the two peristaltic pumps. The control unit was connected via a USB cable to a laptop that allows easy tuning the perfusion flow via a graphical user interface (GUI). The main body of the device is intended to operate inside a standard cell culture incubator to maintain a physiological pH and temperature.

2.2.1. Three-Dimensional-Printed Culture Plates

A set of cultures plates was designed and 3D printed using a Formlabs3 3D printer (Formlabs, Somerville , MA, USA). The culture plate layout was designed by Fusion360 CAD software (Autodesk, San Rafael, CA, USA) and the generated file was exported in a .stl format, imported into PreForm software (Formlabs, Somerville, MA, USA), and 3D printed. The plates were intended to operate independently to allow comparison of two different culture conditions. Holes (1.6 mm in diameter) were placed between adjacent wells to allow a medium flow. The final culture plate layout consists of two 6-well plates made from DentalLT photo-polymer resin (Formlabs, Somerville, MA, USA). This material is approved

for biomedical applications. Culture plates were post-cured using FormWash and FormCure devices (Formlabs, Somerville, MA, USA) following the manufacturer's guidelines.

2.2.2. Graphical User Interface

A user-friendly GUI was implemented in Processing 3 (Processing Foundation, San Diego, CA, USA). This interface allows us to easily administer a perfusion flow rate at three different rates: 0.25, 0.5, and 1 mL/min. Moreover, each perfusion pump can be turned on and off independently. The direction of the rotation can also be set independently. The GUI can be exported to work both on Windows or Mac OS 3.5.4.

2.3. Human Mesenchymal Stem Cell Culture

Primary human bone-marrow-derived mesenchymal stem cells (hBMSCs) were purchased from Lonza Inc. (Allendale, NJ, USA) and used at passage #2 for the seeding onboard 3D scaffolds. A one-week culture followed, either within the bioreactor system or under conventional static conditions as a control. To this aim, the cells were initially expanded as a 2D monolayer in high glucose Dulbecco's Modified Eagle Medium (DMEM) containing 0.1% penicillin/streptomycin, 0.1 mM non-essential amino acids, and 10% fetal bovine serum. After two passages, the hBMSCs were trypsinized and counted in a hemocytometer using Trypan Blue staining to evaluate the number of dead cells. All reagents were purchased from Life Technologies (Carlsbad, CA, USA).

2.4. Cell Culture

hBMSCs at passage #2 were seeded at a concentration of 85,000/50 µL onboard eight 3D chitosan–gelatin–genipin scaffolds (7 mm in height and 5 mm in diameter). Four scaffolds were cultured in either static control or dynamic culture conditions. A 1 mL/min perfusion flow was administered according to [37,38]. To avoid cell loss, scaffold seeding was performed in a 96-well plate, adding over the dry scaffold 50 µL cell solution. Then, 150 µL of medium was added after 2 h.

Osteogenic Differentiation

Scaffolds were moved into the 3D-printed culture plates 36 h after cell seeding.

As shown in Figure 1, the experiment was carried out for eleven days. hMSCs seeded onboard chitosan–gelatin–genipin scaffolds were cultured for five days in 30 mL of proliferative medium per plate. Subsequently, for the next six days, early osteogenic differentiation was induced by adding ascorbic acid, bone morphogenic protein-2 (BMP2), and beta-glicerophosphate to the proliferative medium [39–41]. Half of the exhausted medium (15 mL) was changed every 48 h in both dynamic and static cultures.

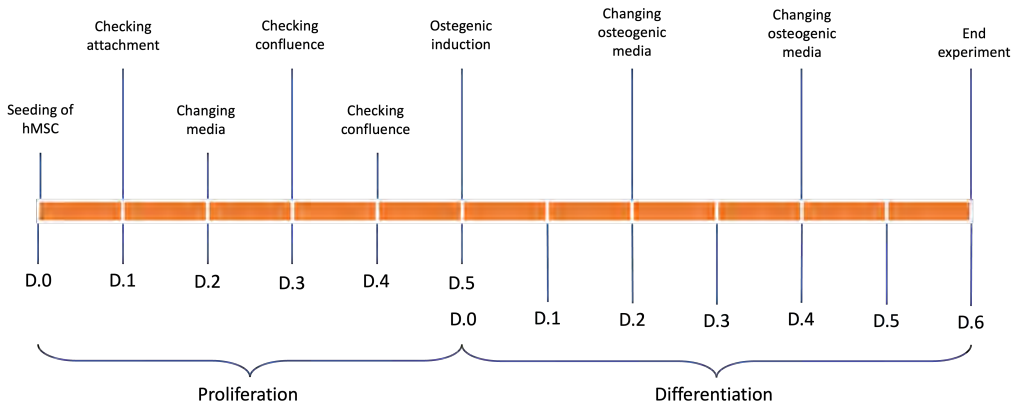

Figure 1. Timeline of experimental setting.

2.5. Micro-Computer Tomography (µCT)

µCT scanning was performed using a SkyScan 1272 micro-computer (Bruker Corporation, Billerica, MA, USA) tomograph at room temperature by rotating the object in front of the source (voltage 45 kV, current 110 mA) for 180 degrees with a rotation step of 0.3 degrees; each frame resulted from an average of 4 projections per frame (550 ms/frame). The scanning resolution (image pixel size) was set at 15 µm for all printed samples. Tomograms were reconstructed from the raw data in Bruker NRecon software (Bruker Corporation, Billerica, MA, USA). Bruker CTAn software (Bruker Corporation, Billerica, MA, USA) was employed to analyze the tomograms and measure the morphological parameters of the printed objects (total porosity, pore/wall size distribution, etc.) and to generate the secondary color-coded dataset depicting pore size variations. All procedures were performed after thresholding (binarization; white pixels for solid sample and black pixels for pores) and despeckling (removal or residual scanning artifacts) and were based on the image pixel size for metric unit conversion.

2.6. Histochemical Assay and Image Analisys

Samples fixed in 4% paraformaldhyde and embedded in paraffin were cut into 5.0 µm thick sections. Samples were stained with hematoxylin and eosin (H&E) for morphological analyses according to [42], and with Alizarin Red S (ARS) to highlight calcium deposits according to [43], indicative of a mineralization process initiated by cells differentiating into an osteogenic phenotype. A quantitative analysis of ECM mineralization (i.e., calcium salt deposits) was performed on images acquired from ARS-stained chitosan–gelatin–genipin scaffold slices. Digital images were acquired in each experimental condition with a Eclipse TE 2000U (Nikon, Tokyo, Japan) optical inverted microscope mounting a 4× Nikon CFI Plan Fluor objective through a DS-5Mc digital camera (Nikon, Tokyo, Japan) operated under a DS-U1 controller connected to a Dell XPS desktop PC equipped with ImageJ (National Institute of Health, Bethesda, MD, USA) image analysis software (version 1.51.m9).

Calcium salt deposits were evaluated in ARS-stained sections using the maximum entropy threshold-based image segmentation method. The count and the average size of the calcium salt deposits, as well the total image area they covered, were calculated. Control (static culture) and dynamic (bioreactor system) data were compared.

3. Results and Discussion

Chitosan/gelatin/genipin (CGG) scaffolds, with an intrinsic characteristic of supporting osteogenic induction in stem cells, were made more efficient through the addition of graphene oxide (GO) [15,44]. Although the properties of this biomaterial have been tested, there is some degree of concern about hypothetical side effects [16]. For this reason, while the results of studies about this issue are pending, we evaluated if a dynamic culture of CGG scaffolds without added GO could increase their osteogenic potential, as heralded in previous work [45–48]. Thus, the in vitro osteogenic potential of the CGG scaffold was investigated in either conventional (i.e., static) or perfusion flow (i.e., dynamic) conditions. The degree of calcium salt deposition by the hBMSCs onboard the 3D scaffold was used as the end-point of the analysis.

3.1. Characterization of CGG Scaffolds

Morphological characterization of the material before cell seeding (i.e., post-synthesis), presented in Figure 2, confirmed the suitability of the CGG scaffold to host the hBMSCs. In detail, qualitative and quantitative analyses were carried out by µCT. Figure 2 shows the 3D reconstruction of a sample scaffold (Figure 2(A1,B1)), as well as the color-coded secondary reconstruction of the pore size (Figure 2(A3,B3)) overlapped with the tomogram of the solid specimen (Figure 2(A2,B2,C)) for a better visualization and comprehension of its intricate pattern and interfaces. The solid sample exhibits a homogeneous architecture, whereby the wall thickness varies to a small extent (with a ratio of more than 99% below 40 µm), contributing to its identification as a consolidated and robust scaffolding material.

However, the pores that are formed span to a broader extent (up to 555 µm), but in a rather balanced Gaussian distribution (Figure 2E). Despite its perceptible solidity, the measured porosity of the freeze-dried material achieves values of 86.8% (Figure 2D); the analysis of pore size domains depicts a great variability that is favorable for both cell lodging and post-adhesion cellular activity, as well as metabolite exchange, supporting these processes for viable tissue construct attainment. The very high incidence (77%) of pores within the range of 120–300 µm could support the employment of this material for transitional total porosity, as it is able to provide accessibility channels for cell nutrients. In addition, the distribution of small pores is extremely homogeneous within the sample (Figure 2, subsets 2, 3), contributing to the interconnected nature of the scaffolding template, a crucial prerequisite of effective materials for tissue regeneration. Furthermore, the surface area of the sample is paramount, especially in the incipient post-seeding stages of cell culture. The surface area of the scanned specimen was measured at 1.11×10^8 µm^2; however, more relevant for material characterization is the specimen-independent measurement of the object surface/volume ratio, which reached the value of 1.97 µm^{-1}.

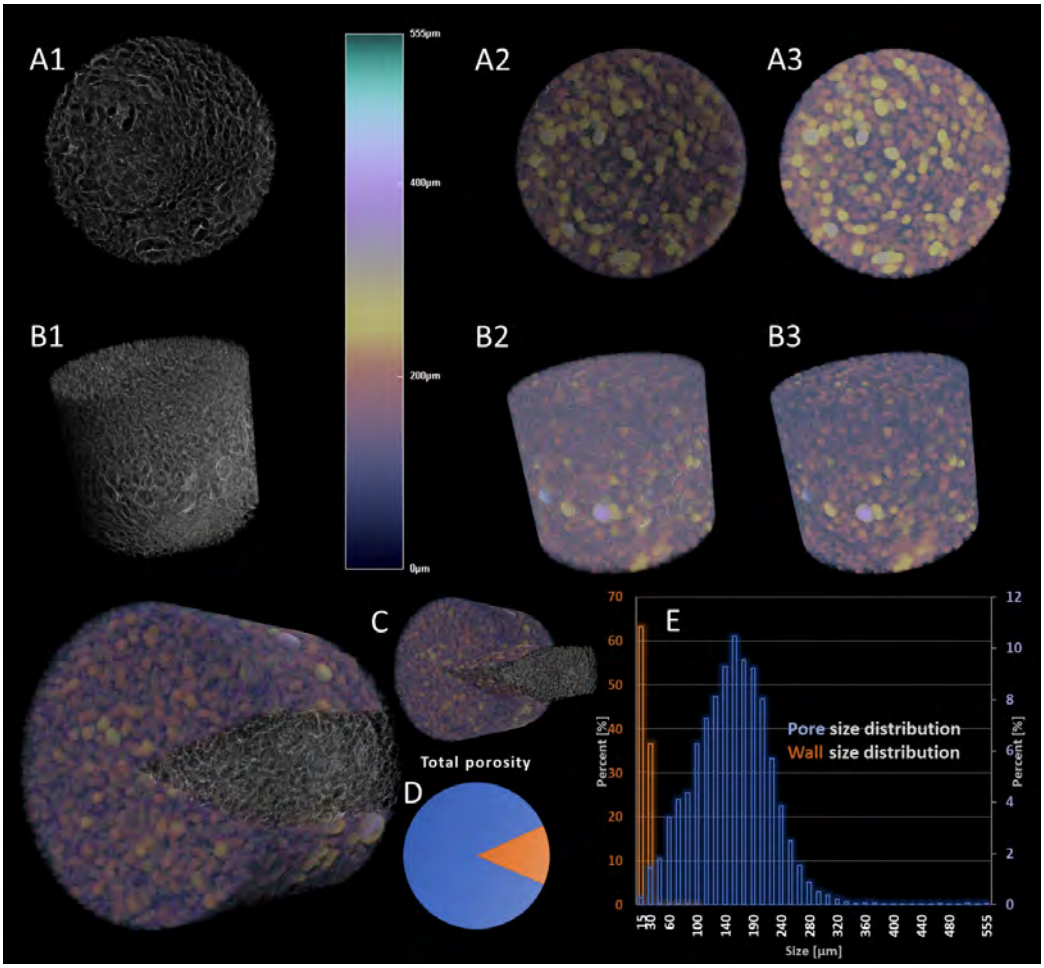

Figure 2. Morphological characterization of chitosan–gelatin–genipin scaffolds by µCT. (**A1**–**A3**) Cross-sectional morphology of the acellular freeze-dried sample; (**B1**–**B3**) overall view of the scanned sample; subset 1, morphology of the solid sample; subset 2, pore reconstruction overlapped to solid objects; subset 3, pore reconstruction and relative pore size according to the color legend. (**C**) Subdivision illustrates a dual view of the solid sample and overlapped pore dataset with the solid. (**D**,**E**) Plot of the pore size and wall thickness distribution.

3.2. Matrix Mineralization upon Dynamic Culture

To overcome the diffusion constraints inherent to a 3D cell culture in a conventional static environment, a custom bioreactor system was used to generate a continuous perfusion flow to sustain cell growth.

Building on our experience in designing and prototyping devices for dynamic culture [37,38,49], we here developed a dedicated tool (Figure 3A) consisting of a unibody plastic case (190 L, 240 W, and 90 H mm in dimensions) and two autoclavable peristaltic pumps acting on two distinct ad hoc culture plates (Figure 3B) and operated by an original graphical user interface (GUI, Figure 3C). This new layout consists of two six-well plates made from DentalLT photo-polymer resin (Formlabs, Somerville, MA, USA) and operated independently to allow comparison of two different culture conditions. In particular, holes (1.6 mm in diameter) were placed between adjacent wells to allow a medium flow.

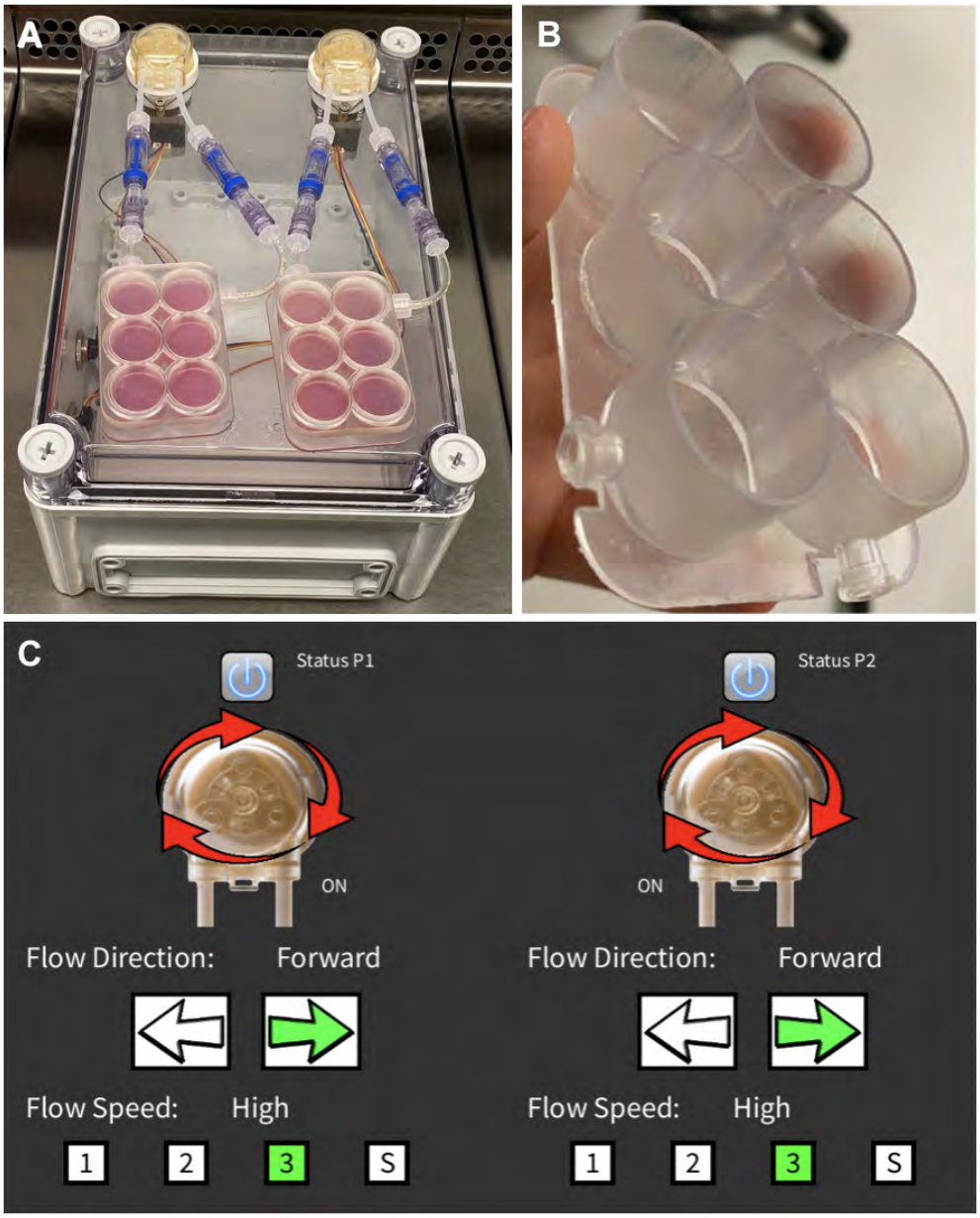

Figure 3. Perfusion bioreactor system overview. (**A**) Perfusion bioreactor; (**B**) Six-well plate; (**C**) Graphical user interface (GUI): peristaltic pumps (P1 and P2) status (ON/OFF), flow direction, and flow speed.

Figure 4A,B shows the viability and distribution of the hBMSCs seeded in the 3D CGG scaffolds. Hematoxylin/eosin staining analysis highlighted a higher amount of cells (purple spots) in dynamic conditions (Figure 4B) compared to static conditions (Figure 4A). Figure 4C,D shows that 3D-perfused CGG scaffolds display enhanced levels of extracellular matrix (ECM) mineralization, suggesting an early osteogenic commitment. In fact, alizarin red S staining analysis highlighted a higher amount of calcium deposits (black spots) in dynamic conditions (Figure 4D) compared to static conditions (Figure 4C). For both analyses, a remodelling of the scaffold structure was observed when hBMSCs were cultured in dynamic conditions, resulting in thickening of the scaffold texture.

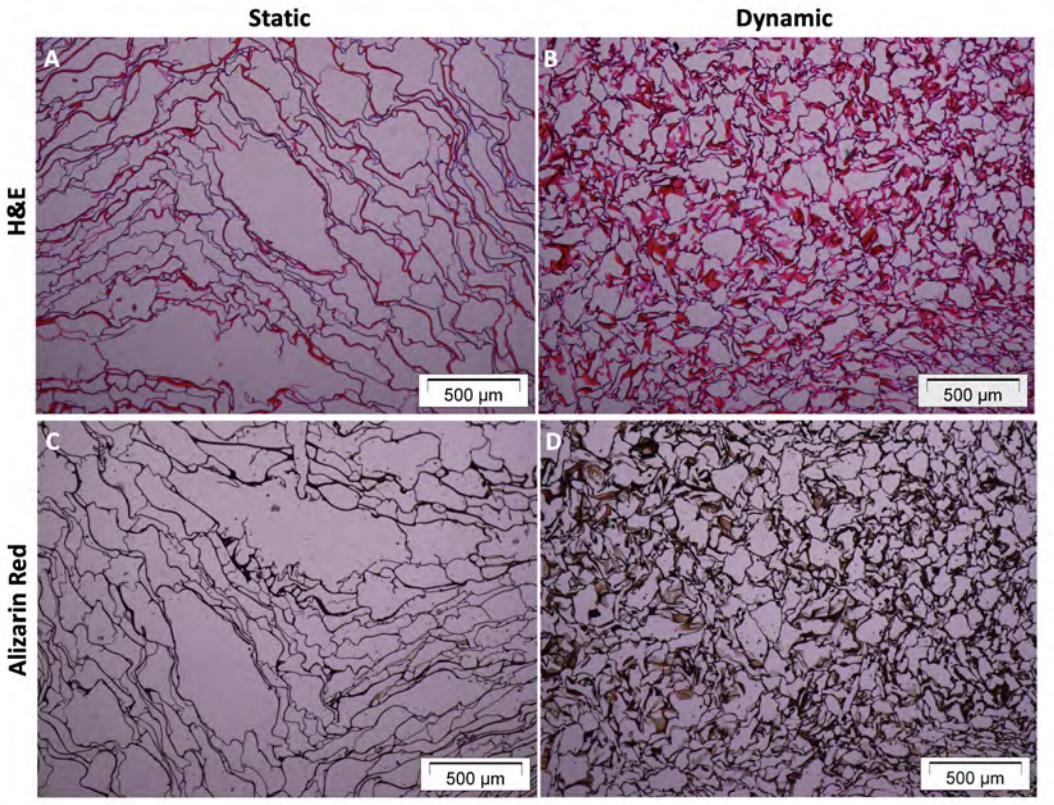

Figure 4. Histological analysis of the 3D chitosan–gelatin–genipin scaffold seeded with hBMSCs and subjected to six days of osteogenic induction. (**A**,**B**) Hematoxylin and eosin assay on scaffolds cultured in static (**A**) vs. dynamic (**B**) conditions; (**C**,**D**) Alizarin Red S assay on scaffolds cultured in static (**C**) vs. dynamic (**D**) conditions. Pictures acquired at 40× magnification, using Cell^A Software (version 2.5). Scale bar 500 µm.

A detailed quantification of the calcium salt deposit amount, carried out through the maximum entropy threshold-based image segmentation method, is presented in Figure 5. In particular, Figure 5B shows the segmented area referring to the calcium salt deposition over the 3D CGG scaffold fibers by the hBMSCs when cultured under static condition (Figure 5A). Figure 5D shows the segmented area referring to the calcium salt deposition over the 3D CGG scaffold fibers by the hBMSCs when cultured under dynamic conditions (Figure 5C).

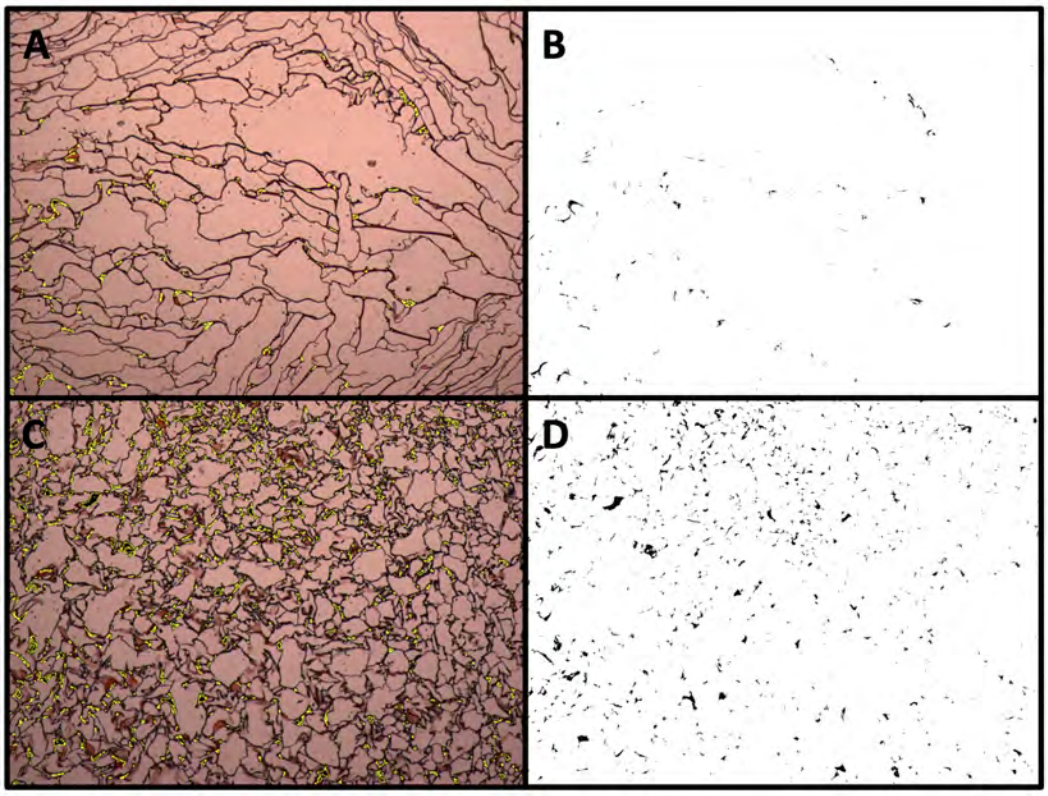

Figure 5. Quantification of calcium deposits using alizarin red S staining. (**A**) Static conditions; (**C**) dynamic conditions; (**B**,**D**) segmented areas of the calcium salt deposits.

The amount of scaffold area covered by the calcium salt deposits in both static and dynamic conditions is reported in Table 1. The results are reported as the count and average size of the calcium salts, as well as the total image area covered. Higher values were obtained for 3D CGG scaffolds cultured in dynamic conditions.

Table 1. Amount of scaffold area covered by the calcium salts.

Slice	Count	Total Area	Average Size
ARS Static	892	0.610	6.837×10^{-4}
ARS Dynamic	4754	6.730	0.001

4. Conclusions

The purpose of this work was to improve the osteogenic potential of chitosan/gelatin/genipin (CGG) scaffolds without added graphene oxide (GO) by including a perfusion flow into the differentiating protocol of human bone-marrow-derived stem cells seeded onboard the scaffold. A histological analysis showed enhanced extracellular matrix mineralization under a perfusion flow in an osteogenic medium, suggesting an early osteogenic commitment. The results of this investigation reveal a new perspective on potential clinical applications of CGG scaffolds without added GO.

Author Contributions: Conceptualization, J.L.; methodology, J.L. and G.B.; software, G.B.; formal analysis, G.B. and G.M.V.; investigation, J.L., G.B. and G.M.V.; resources, J.L., Ó.E.S. and P.G.; data curation, J.L., G.B. and G.M.V.; writing—original draft preparation, J.L., G.B. and E.G.; writing—review and editing, J.L., E.G., M.I., Ó.E.S. and P.G.; supervision, J.L. and Ó.E.S.; project administration, J.L.; funding acquisition, J.L. All authors have read and agreed to the published version of the manuscript.

Funding: This research was funded by the Icelandic Centre for Research (RANNIS), grant number 228340-051.

Conflicts of Interest: The authors declare no conflict of interest. The funders had no role in the design of the study; in the collection, analyses, or interpretation of data; in the writing of the manuscript; or in the decision to publish the results.

References

1. Valtanen, R.S.; Yang, Y.P.; Gurtner, G.C.; Maloney, W.J.; Lowenberg, D.W. Synthetic and Bone Tissue Engineering Graft Substitutes: What Is the Future? *Injury* **2021**, *52*, S72–S77. [CrossRef] [PubMed]
2. Qi, J.; Yu, T.; Hu, B.; Wu, H.; Ouyang, H. Current Biomaterial-Based Bone Tissue Engineering and Translational Medicine. *Int. J. Mol. Sci.* **2021**, *22*, 10233. [CrossRef]
3. Roseti, L.; Parisi, V.; Petretta, M.; Cavallo, C.; Desando, G.; Bartolotti, I.; Grigolo, B. Scaffolds for Bone Tissue Engineering: State of the art and new perspectives. *Mater. Sci. Eng. C Mater. Biol. Appl.* **2017**, *78*, 1246–1262. [CrossRef]
4. Khan, Y.; Yaszemski, M.J.; Mikos, A.G.; Laurencin, C.T. Tissue engineering of bone: Material and matrix considerations. *J. Bone Jt. Surg. Am.* **2008**, *90* (Suppl. S1), 36–42. [CrossRef]
5. Tang, D.; Tare, R.S.; Yang, L.-Y.; Williams, D.F.; Ou, K.-L.; Oreffo, R.O.C. Biofabrication of Bone Tissue: Approaches, Challenges and Translation for Bone Regeneration. *Biomaterials* **2016**, *83*, 363–382. [CrossRef]
6. Filippi, M.; Born, G.; Chaaban, M.; Scherberich, A. Natural Polymeric Scaffolds in Bone Regeneration. *Front. Bioeng. Biotechnol.* **2020**, *8*, 474. [CrossRef]
7. El-Fiqi, A.; Kim, J.H.; Kim, H.W. Novel bone-mimetic nanohydroxyapatite/collagen porous scaffolds biomimetically mineralized from surface silanized mesoporous nanobioglass/collagen hybrid scaffold: Physicochemical, mechanical and in vivo evaluations. *Mater. Sci. Eng. C Mater. Biol. Appl.* **2020**, *110*, 110660. [CrossRef]
8. Silva, J.C.; Carvalho, M.S.; Udangawa, R.N.; Moura, C.S.; Cabral, J.M.S.; Lda Silva, C.; Ferreira, F.C.; Vashishth, D.; Linhardt, R.J. Extracellular Matrix Decorated Polycaprolactone Scaffolds for Improved Mesenchymal Stem/Stromal Cell Osteogenesis towards a Patient-tailored Bone Tissue Engineering Approach. *J. Biomed. Mater. Res. Part B Appl. Biomater.* **2020**, *108*, 2153–2166. [CrossRef]
9. Wu, Z.; Meng, Z.; Wu, Q.; Zeng, D.; Guo, Z.; Yao, J.; Bian, Y.; Gu, Y.; Cheng, S.; Peng, L.; et al. Biomimetic and Osteogenic 3D Silk Fibroin Composite Scaffolds with Nano MgO and Mineralized Hydroxyapatite for Bone Regeneration. *J. Tissue Eng.* **2020**, *11*, 204173142096779. [CrossRef]
10. Lai, Y.; Li, Y.; Cao, H.; Long, J.; Wang, X.; Li, L.; Li, C.; Jia, Q.; Teng, B.; Tang, T.; et al. Osteogenic Magnesium Incorporated into PLGA/TCP Porous Scaffold by 3D Printing for Repairing Challenging Bone Defect. *Biomaterials* **2019**, *197*, 207–219. [CrossRef]
11. Xie, H.; Wang, Z.; Zhang, L.; Lei, Q.; Zhao, A.; Wang, H.; Li, Q.; Cao, Y.; Jiezhang, W.; Chen, Z. Extracellular Vesicle-Functionalized Decalcified Bone Matrix Scaffolds with Enhanced Pro-Angiogenic and Pro-Bone Regeneration Activities. *Sci. Rep.* **2017**, *7*, 45622. [CrossRef]
12. Saravanan, S.; Leena, R.S.; Selvamurugan, N. Chitosan based biocomposite scaffolds for bone tissue engineering. *Int. J. Biol. Macromol.* **2016**, *93 Pt B*, 1354–1365. [CrossRef]
13. Sukpaita, T.; Chirachanchai, S.; Pimkhaokham, A.; Ampornaramveth, R.S. Chitosan-Based Scaffold for Mineralized Tissues Regeneration. *Mar. Drugs* **2021**, *19*, 551. [CrossRef]
14. Chang, P.H.; Chao, H.M.; Chern, E.; Hsu, S.H. Chitosan 3D cell culture system promotes naïve-like features of human induced pluripotent stem cells: A novel tool to sustain pluripotency and facilitate differentiation. *Biomaterials* **2021**, *268*, 120575. [CrossRef]
15. Șelaru, A.; Herman, H.; Vlăsceanu, G.M.; Dinescu, S.; Gharbia, S.; Baltă, C.; Roșu, M.; Mihali, C.V.; Ioniță, M.; Serafim, A.; et al. Graphene–Oxide Porous Biopolymer Hybrids Enhance In Vitro Osteogenic Differentiation and Promote Ectopic Osteogenesis In Vivo. *Int. J. Mol. Sci.* **2022**, *23*, 491. [CrossRef]
16. Chiticaru, E.A.; Ionita, M. Graphene Toxicity and Future Perspectives in Healthcare and Biomedicine. *FlatChem* **2022**, *35*, 100417. [CrossRef]
17. Holt, B.D.; Wright, Z.M.; Arnold, A.M.; Sydlik, S.A. Graphene oxide as a scaffold for bone regeneration. *Wiley Interdiscip. Rev. Nanomed. Nanobiotechnol.* **2017**, *9*, e1437. [CrossRef]
18. Ranganathan, S.; Balagangadharan, K.; Selvamurugan, N. Chitosan and gelatin-based electrospun fibers for bone tissue engineering. *Int. J. Biol. Macromol.* **2019**, *133*, 354–364. [CrossRef]
19. Muzzarelli, R.A.; El Mehtedi, M.; Bottegoni, C.; Aquili, A.; Gigante, A. Genipin-Crosslinked Chitosan Gels and Scaffolds for Tissue Engineering and Regeneration of Cartilage and Bone. *Mar. Drugs* **2015**, *13*, 7314–7338. [CrossRef]
20. Lovecchio, J.; Pannella, M.; Giardino, L.; Calzà, L.; Giordano, E. A Dynamic Culture Platform Enhances the Efficiency of the 3D HUVEC-based Tube Formation Assay. *Biotechnol. Bioeng.* **2019**, *117*, 789–797. [CrossRef]
21. Ciardulli, M.C.; Marino, L.; Lovecchio, J.; Giordano, E.; Forsyth, N.R.; Selleri, C.; Maffulli, N.; Porta, G.D. Tendon and Cytokine Marker Expression by Human Bone Marrow Mesenchymal Stem Cells in a Hyaluronate/Poly-Lactic-Co-Glycolic Acid (PLGA)/Fibrin Three-Dimensional (3D) Scaffold. *Cells* **2020**, *9*, 1268. [CrossRef] [PubMed]
22. Lamparelli, E.P.; Lovecchio, J.; Ciardulli, M.C.; Giudice, V.; Dale, T.P.; Selleri, C.; Forsyth, N.; Giordano, E.; Maffulli, N.; Della Porta, G. Chondrogenic Commitment of Human Bone Marrow Mesenchymal Stem Cells in a Perfused Collagen Hydrogel Functionalized with HTGF-β1-Releasing PLGA Microcarrier. *Pharmaceutics* **2021**, *13*, 399. [CrossRef]

23. Rauh, J.; Milan, F.; Günther, K.P.; Stiehler, M. Bioreactor systems for bone tissue engineering. *Tissue Eng. Part B Rev.* **2011**, *17*, 263–280. [CrossRef] [PubMed]
24. Bancroft, G.N.; Sikavitsas, V.I.; Mikos, A.G. Design of a flow perfusion bioreactor system for bone tissue-engineering applications. *Tissue Eng.* **2003**, *9*, 549–554. [CrossRef] [PubMed]
25. Gaspar, D.A.; Gomide, V.; Monteiro, F.J. The role of perfusion bioreactors in bone tissue engineering. *Biomatter* **2012**, *2*, 167–175. [CrossRef] [PubMed]
26. Yeatts, A.B.; Fisher, J.P. Bone tissue engineering bioreactors: Dynamic culture and the influence of shear stress. *Bone* **2011**, *48*, 171–181. [CrossRef]
27. Qi, P.; Ning, Z.; Zhang, X. Synergistic effects of 3D chitosan-based hybrid scaffolds and mesenchymal stem cells in orthopaedic tissue engineering. *IET Nanobiotechnol.* **2023**, *17*, 41–48. [CrossRef] [PubMed]
28. Chiono, V.; Pulieri, E.; Vozzi, G.; Ciardelli, G.; Ahluwalia, A.; Giusti, P. Genipin-crosslinked chitosan/gelatin blends for biomedical applications. *J. Mater. Sci. Mater. Med.* **2008**, *19*, 889–898. [CrossRef] [PubMed]
29. Siddiqui, N.; Pramanik, K.; Jabbari, E. Osteogenic differentiation of human mesenchymal stem cells in freeze-gelled chitosan/nano β-tricalcium phosphate porous scaffolds crosslinked with genipin. *Mater. Sci. Eng. C Mater. Biol. Appl.* **2015**, *54*, 76–83. [CrossRef] [PubMed]
30. Meinel, L.; Karageorgiou, V.; Fajardo, R.; Snyder, B.; Shinde-Patil, V.; Zichner, L.; Kaplan, D.; Langer, R.; Vunjak-Novakovic, G. Bone tissue engineering using human mesenchymal stem cells: Effects of scaffold material and medium flow. *Ann. Biomed. Eng.* **2004**, *32*, 112–122. [CrossRef] [PubMed]
31. Bruder, S.P.; Fink, D.J.; Caplan, A.I. Mesenchymal stem cells in bone development, bone repair, and skeletal regeneration therapy. *J. Cell Biochem.* **1994**, *5*, 283–294. [CrossRef]
32. Qin, Y.; Guan, J.; Zhang, C. Mesenchymal stem cells: Mechanisms and role in bone regeneration. *Postgrad. Med. J.* **2014**, *90*, 643–647. [CrossRef]
33. Janfada, A.; Asefnejad, A.; Khorasani, M.T.; Joupari, M.D. Reinforcement of Electrospun Polycaprolacton Scaffold Using KIT-6 to Improve Mechanical and Biological Performance. *Polym. Test.* **2020**, *84*, 106391. [CrossRef]
34. Zhao, F.; Van Rietbergen, B.; Ito, K.; Hofmann, S. Flow rates in perfusion bioreactors to maximise mineralisation in bone tissue engineering in vitro. *J. Biomech.* **2018**, *79*, 232–237. [CrossRef]
35. Grayson, W.L.; Bhumiratana, S.; Cannizzaro, C.; Chao, P.H.; Lennon, D.P.; Caplan, A.I.; Vunjak-Novakovic, G. Effects of initial seeding density and fluid perfusion rate on formation of tissue-engineered bone. *Tissue Eng. Part A* **2008**, *14*, 1809–1820. [CrossRef]
36. Zhao, F.; Ma, T. Perfusion bioreactor system for human mesenchymal stem cell tissue engineering: Dynamic cell seeding and construct development. *Biotechnol. Bioeng.* **2005**, *91*, 482–493. [CrossRef]
37. Pasini, A.; Lovecchio, J.; Ferretti, G.; Giordano, E. Medium Perfusion Flow Improves Osteogenic Commitment of Human Stromal Cells. *Stem Cells Int.* **2019**, *2019*, 1304194. [CrossRef]
38. Lovecchio, J.; Gargiulo, P.; Vargas Luna, J.L.; Giordano, E.; Sigurjónsson, Ó.E. A Standalone Bioreactor System to Deliver Compressive Load under Perfusion Flow to HBMSC-Seeded 3D Chitosan-Graphene Templates. *Sci. Rep.* **2019**, *9*, 16854. [CrossRef]
39. Fiorentini, E.; Granchi, D.; Leonardi, E.; Baldini, N.; Ciapetti, G. Effects of osteogenic differentiation inducers on in vitro expanded adult mesenchymal stromal cells. *Int. J. Artif. Organs* **2011**, *34*, 998–1011. [CrossRef]
40. Anselme, K.; Broux, O.; Noel, B.; Bouxin, B.; Bascoulergue, G.; Dudermel, AF.; Bianchi, F.; Jeanfils, J.; Hardouin, P. In vitro control of human bone marrow stromal cells for bone tissue engineering. *Tissue Eng.* **2002**, *8*, 941–953. [CrossRef]
41. Langenbach, F.; Handschel, J. Effects of dexamethasone, ascorbic acid and β-glycerophosphate on the osteogenic differentiation of stem cells in vitro. *Stem Cell Res. Ther.* **2013**, *4*, 117. [CrossRef]
42. Fischer, A.H.; Jacobson, K.A.; Rose, J.; Zeller, R. Hematoxylin and eosin staining of tissue and cell sections. *CSH Protoc.* **2008**, *2008*, pdb.prot4986. [CrossRef]
43. Puchtler, H.; Meloan, S.N.; Terry, M,S. On the history and mechanism of alizarin and alizarin red S stains for calcium. *J. Histochem. Cytochem.* **1969**, *17*, 110–124. [CrossRef] [PubMed]
44. Vlasceanu, G.M.; Șelaru, A.; Dinescu, S.; Balta, C.; Herman, H.; Gharbia, S.; Hermenean, A.; Ionita, M.; Costache, M. Comprehensive Appraisal of Graphene–Oxide Ratio in Porous Biopolymer Hybrids Targeting Bone-Tissue Regeneration. *Nanomaterials* **2020**, *10*, 1444. [CrossRef]
45. Kronstadt, S.M.; Patel, D.B.; Born, L.J.; Levy, D.; Lerman, M.J.; Mahadik, B.; McLoughlin, S.T.; Fasuyi, A.; Fowlkes, L.; Van Heyningen, L.H.; et al. Mesenchymal Stem Cell Culture within Perfusion Bioreactors Incorporating 3D-Printed Scaffolds Enables Improved Extracellular Vesicle Yield with Preserved Bioactivity. *Adv. Healthc. Mater.* **2023**, *2023*, 2300584. [CrossRef] [PubMed]
46. Schröder, M.; Reseland, J.E.; Haugen, H.J. Osteoblasts in a Perfusion Flow Bioreactor—Tissue Engineered Constructs of TiO_2 Scaffolds and Cells for Improved Clinical Performance. *Cells* **2022**, *11*, 1995. [CrossRef] [PubMed]
47. Yamada, S.; Yassin, M.A.; Schwarz, T.; Mustafa, K.; Hansmann, J. Optimization and Validation of a Custom-Designed Perfusion Bioreactor for Bone Tissue Engineering: Flow Assessment and Optimal Culture Environmental Conditions. *Front. Bioeng. Biotechnol.* **2022**, *10*, 811942. [CrossRef] [PubMed]

48. Kleinhans, C.; Mohan, R.R.; Vacun, G.; Schwarz, T.; Haller, B.; Sun, Y.; Kahlig, A.; Kluger, P.; Finne-Wistrand, A.; Walles, H.; et al. A Perfusion Bioreactor System Efficiently Generates Cell-loaded Bone Substitute Materials for Addressing Critical Size Bone Defects. *Biotechnol. J.* **2015**, *10*, 1727–1738. [CrossRef]
49. Lovecchio J.; Jónsdóttir-Buch, S.M.; Einarsdóttir G.K.; Gíslason M.K.; Örlygsson G.; Sigurjónsson Ó.E.; Gargiulo P. Assessment of a Perfusion Bioreactors System using μCT Technology and 3D Modeling Methods. *Biomed. Eng./Biomed. Tech.* **2014**, *59*, S302–S305. [CrossRef]